Phosphor-converted LED modeling by bidirectional photometric data

Chien-Hsiang Hung[1], Chung-Hao Tien[2]

[1] *Department of Photonics and Institute of Electro-optical Engineering, National Chiao Tung University, Hsinchu 30010, Taiwan*

[2] *Department of Photonics and Display Institute, National Chiao Tung University, Hsinchu 30010, Taiwan*

Abstract: For the phosphor-converted light-emitting diodes (pcLEDs), the interaction of the illuminating energy with the phosphor would not just behave as a simple wavelength-converting phenomenon, but also a function of various combinations of illumination and viewing geometries. This paper presents a methodology to characterize the converting and scattering mechanisms of the phosphor layer in the pcLEDs by the measured bidirectional scattering distribution functions (BSDFs). A commercially available pcLED with conformal phosphor coating was used to examine the validity of the proposed model. The close agreement with the measurement illustrates that the proposed characterization opens new perspectives for phosphor-based conversion and scattering feature for white lighting uses.

OCIS codes: (120.5820) Scattering measurements; (290.1483) BSDF, BRDF, and BSDF; (230.3670) Light-emitting diodes

References and links

1. S. Nakamura, and G. Fasol, *The Blue Laser Diode: GaN Based Light Emitters and Lasers*, (Springer-Verlag, New York, 1997).
2. R. Mueller-Mach, G. O. Mueller, M. R. Krames, and T. Trottier, "High-power phosphor-converted light-emitting diodes based on III-nitrides," IEEE J. Sel. Top. Quantum Electron. **8**(2), 339–345 (2002).
3. http://www.philipslumileds.com/technology/whitelighting.cfm
4. N. Narendran, Y. Gu, J. P. Freyssinier-Nova, and Y. Zhu, "Extracting phosphor-scattered photons to improve white LEDs efficiency," Phys. Stat. Solid A **202**(6), R60–R62 (2005).
5. H. Luo, J. K. Kim, E. F. Schubert, J. Cho, C. Sone, and Y. Park, "Analysis of high-power packages for phosphor based white-light-emitting diodes," Appl. Phys. Lett. **86**(24), 243505 (2005).
6. Y. Ito, T. Tsukahara, S. Masuda, T. Yoshida, N. Nada, T. Igarashi, T. Kusunoki, and J. Ohsako, "Optical design of phosphor sheet structure in LED backlight system," SID Int. Symp. Digest Tech. Papers **39**(1), 866–869 (2008).
7. C.-H. Tien, C.-H. Hung, B.-W. Xiao, H.-T. Huang, Y.-P. Huang, and C.-C. Tsai, "Planar lighting by blue LEDs array with remote phosphor," Proc. SPIE **7617**, 761707 (2010).
8. S. C. Allen, and A. J. Steckl, "ELiXIR—Solid-state luminaire with enhanced light extraction by internal reflection," J. Disp. Technol. **3**(2), 155–159 (2007).
9. S. C. Allen, and A. J. Steckl, "A nearly ideal phosphor-converted white light-emitting diode," Appl. Phys. Lett. **92**(14), 143309 (2008).
10. K. Yamada, Y. Imai, and K. Ishi, "Optical simulation of light source devices composed of blue LEDs and YAG phosphor," J. Light Vis. Env. **27**(2), 70–74 (2003).
11. Y. Zhu, N. Narendran, and Y. Gu, "Investigation of the optical properties of YAG: Ce phosphor," Proc. SPIE **6337** (2006).
12. Commission Internationale de l'Eclairage, *Radiometric and Photometric Characteristics of Materials and their Measurement, 2ndEdition*, (CIE 38 (TC-2.3), Paris, 1977).
13. F. E. Nicodemus, J. C. Richmond, J. J. Hsia, I. W. Ginsberg, and T. Limperis, *Geometrical Considerations and Nomenclature for Reflectance*, (National Bureau of Standards (US), 1977), Monograph 160.
14. X. Francois Sillion, and Claude Puech, *Radiosity and Global Illumination*, (Morgan Kaufmann Publishers Inc., San Francisco, 1994).
15. J. de Boer, "Modelling indoor illumination by complex fenestration systems based on bidirectional photometric data," Energy Build. **38**(7), 849–868 (2006).
16. C.-H. Tien, and C.-H. Hung, "An iterative model of diffuse illumination from bidirectional photometric data," Opt. Express **17**(2), 723–732 (2009).
17. M. E. Becker, "Evaluation and characterization of display reflectance," Displays **19**(1), 35–54 (1998).
18. M. E. Becker, "Display Reflectance: Basics, Measurement, and Rating," J. SID **14**(11), 1003–1017 (2006).

#124178 - $15.00 USD Received 11 Feb 2010; revised 21 May 2010; accepted 7 Jun 2010; published 24 Jun 2010

19. H.-T. Huang, C.-C. Tsai, Y.-P. Huang, J. Chen, J. Lin, and W.-C. Chang, "Phosphor conformal coating by a novel spray method for white light-emitting diodes as applied to liquid-crystal backlight module," in *proc. International Display Research Conference* (Rome, Italy, 2009) 17.5.
20. M. Shaw, and T. Goodman, "Array-based goniospectroradiometer for measurement of spectral radiant intensity and spectral total flux of light sources," Appl. Opt. **47**(14), 2637–2647 (2008).

1. Introduction

The wavelength converting schemes have been widely used in many illuminating subjects, including cold cathode fluorescent lamps (CCFLs), plasma emission devices, and phosphor-converted light-emitting diodes (pcLEDs). Over the variety of applications, the rapid progress of pcLEDs has attracted much attention due to the emerging LED lighting market. The most general pcLED schemes use the broadband yellow phosphor (yttrium aluminum garnet: YAG) to absorb the blue-light flux from a GaN chip and generate the white light by mixing the die-emitted blue light with the phosphor-converted yellow light [1]. In additional to the phosphor improvement, the configuration of pcLEDs was also evolved from the conventional scheme, where the YAG powder phosphor is directly coated on the GaN surface [2,3], to the remote phosphor approaches. The separation of the phosphor from the LED surface was firstly proposed as the scattered photon extraction (SPE) structure by *N. Narendran* et al. to enhance the extraction efficiency [4]. After that, the multi-functional consideration including the remote phosphor, diffuse reflector cup, and hemispherical dome was further designed to minimize the guided radiant flux inside the LED [5]. The concepts of the remote phosphor separated by an air gap from the blue LED were addressed to achieve various targets, such as highly uniform planar source [6,7], and enhanced light extraction by internal reflection [8,9].

The phosphor material absorbs energy in a region of wavelengths and then re-emits the energy in a region of longer wavelengths. In terms of the pcLEDs, because the phosphor-scattered blue light and phosphor-emitted yellow light have different radiant intensity distributions, there is a non-uniform angular color distribution. Few studies have attempted to characterize the optical properties of the YAG phosphor in the pcLEDs due to the massive quantities of measurement and underlying complicated physical processes. K. Yamada et al. simulated the YAG phosphor film in a pcLED by defining the transmitted and reflected flux of the blue and yellow light, respectively [10]. Although they analyzed the pcLED structure by the optical simulation with the measured phosphor properties, the accuracy of the simulated results was not verified. Zhu et al. also used two integrating spheres to measure the amount of transmitted and reflected power for characterizing the optical throughput of a YAG phosphor slide, which was illuminated by a fiber-guided source [11]. However, the interaction of the illuminating energy with the phosphor would not just behave as a simple wavelength-converting phenomenon, but also a function of the illuminating and viewing geometry. In other words, the description of the phosphor-light interaction shall be associated with wavelength as well as geometric considerations, which can't be merely defines by the transmitted or reflected flux. Furthermore, the fiber-produced light sources in the references are not appropriate to be involved as the LED chip-emitted field. A general and complete description of such wavelength-converting properties should be defined for the incident light fields of the various LED configurations.

In this study, we propose a simple but effective methodology to characterize the optical properties of the phosphor layer in the pcLEDs by using the measured bidirectional scattering distribution functions (BSDFs), which are regarded as the angular impulse responses of a phosphor layer. The BSDF characterization can completely describe the energy relation of the direction and wavelength. The characterizing methodology and its measurement are introduced. Finally, a commercially available pcLED with the conformal phosphor coating was examined to validate the proposed methodology accordingly.

#124178 - $15.00 USD Received 11 Feb 2010; revised 21 May 2010; accepted 7 Jun 2010; published 24 Jun 2010

2. Phosphor characterization

2.1 Energy balance equation

To characterize the phosphor in a pcLED sample, the BSDFs was adopted to define the general description of light propagation with the angular and wavelength variables [12, 13]. However, the optical properties are prohibitively complicated and lead to massive quantities of data. In order to avoid the explosion of photometric data, some conditions were assumed:

1. The geometrical configuration of phosphor is treated as a thin-layer approximation, including a forward and backward surface related to the LED chip.
2. The optical features of the phosphor include the wavelength conversion and scatter.
3. The relation of the incident and outgoing flux satisfies scalability and addictivity due to the linear conversion between the LED-emitted and phosphor-emitted spectral power distribution.

In this paper, the forward mode was expressed in the equations. The associated photometric and geometric quantities in polar coordinates are illustrated in Fig. 1, where all the scientific symbols and terminology through this paper are listed in Table 1.

First of all, the energy balance equation [14] for a radiating surface is expressed by the following equation:

$$\underbrace{L(x,y,\theta_t,\phi_t)}_{\text{total radiance}} = \underbrace{L_s(x,y,\theta_t,\phi_t)}_{\text{non-emitted radiance}} + \underbrace{L_e(x,y,\theta_t,\phi_t)}_{\text{emitted radiance}}, \tag{1}$$

where L, L_e, and L_s are the total radiance, the emitted radiance, and the non-emitted (scattered) radiance leaving point (x, y) in transmitting-side direction (θ_t, ϕ_t). Here we assume that the phosphor layer is homogenous, the position (x, y) is not included as parameter. Based on the wavelength conversion mechanisms of pcLEDs, the energy balance equation of the phosphor is composed of three terms:

$$\begin{aligned} L(\theta_t,\phi_t) &= L_{fs}^{B}(\theta_t,\phi_t) + L_{fe}^{Y}(\theta_t,\phi_t) + L_{fs}^{Y}(\theta_t,\phi_t) \\ &= \int_{\Omega_i} \left[(\rho_{fs}^{B-B} + \rho_{fe}^{B-Y}) L_i^{B}(\theta_i,\phi_i) + \rho_{fs}^{Y-Y} L_i^{Y}(\theta_i,\phi_i) \right] \cos\theta_i d\omega_i, \end{aligned} \tag{2}$$

where L_{fs}^{B}, L_{fe}^{Y}, and L_{fs}^{Y} indicate the forward-scattered blue-light, forward-emitted yellow-light, and forward-scattered yellow-light radiance, respectively. As the equation shows, the three transmitting radiance terms are obtained by the integration of the incident blue-light radiance L_i^{B} and yellow-light radiance L_i^{Y} over the full solid angle Ω_i of the incident hemisphere. Here the weights, $\rho_{fs}^{B\text{-}B}$, $\rho_{fe}^{B\text{-}Y}$, and $\rho_{fs}^{Y\text{-}Y}$, represent the bidirectional photometric data with blue-to-blue, blue-to-yellow, and yellow-to-yellow pairs, respectively.

#124178 - $15.00 USD Received 11 Feb 2010; revised 21 May 2010; accepted 7 Jun 2010; published 24 Jun 2010

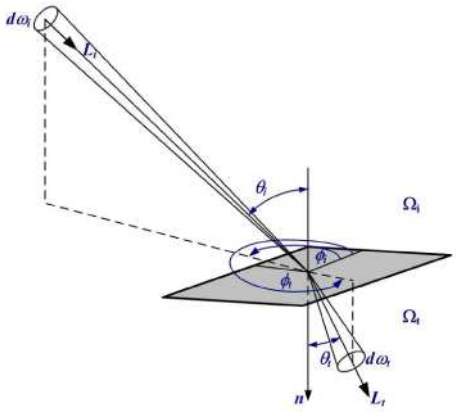

Fig. 1. Photometric and geometric quantities in the polar coordinate system.

Table 1. Nomenclature

Abbreviations		Subscripts and superscripts	
L	radiance (W/sr*m^2)	***i***	Incident
I	radiant intensity (W/sr)	***t***	Transmitted
Φ	light flux (W)	***B***	blue light
P	spectral radiance (W/sr*m^3)	***Y***	yellow light
P	bidirectional function (sr^{-1})	***fs***	forward scattered
***ω*, Ω**	solid angle (sr)	***fe***	forward emitted
θ*, *ϕ	polar coordinates	***bs***	backward scattered
Λ	wavelength	***be***	backward emitted

2.2 Blue-to-blue radiance L_{fs}^{B}

In terms of the non-emitted radiance, the forward scattered blue-light radiance, L_{fs}^{B}, is determined by the incident radiance L_i^B and blue-to-blue bidirectional distribution function $\rho_{fs}^{B\text{-}B}$,

$$L_{fs}^{B}(\theta_t,\phi_t) = \int_{\Omega_i} \rho_{fs}^{B-B}(\theta_i,\phi_i,\theta_t,\phi_t) L_i^B(\theta_i,\phi_i)\cos\theta_i d\omega_i, \tag{3}$$

where $\rho_{fs}^{B\text{-}B}$ is defined by the ratio of the transmitted radiance dL_{fs}^{B} in the transmitted direction (θ_t, ϕ_t) to the irradiance dE_i^B in an incident direction (θ_i, ϕ_i),

$$\rho_{fs}^{B-B}(\theta_i,\phi_i,\theta_t,\phi_t) = \frac{dL_{fs}^{B}(\theta_t,\phi_t)}{dE_i^B(\theta_i,\phi_i)} = \frac{dL_{fs}^{B}(\theta_t,\phi_t)}{L_i^B(\theta_i,\phi_i)\cos\theta_i d\omega_i}. \tag{4}$$

For pcLEDs, the GaN LED serves as the excitation source with a specific spectral power distribution $P_i^B(\lambda)$. In terms of blue-to-blue radiance, the role of phosphor is a typical scattering material. Thus, the phosphor-scattered radiance has a spectral power distribution $P_{fs}^{B}(\lambda)$ which is identical to that of the incident light peaking around 450 nm. Figure 2 shows the normally incident spectrum $P_i^B(\lambda)$ of illumination and the transmitted spectrum $P_{fs}^{B}(\lambda)$ detected in the normal direction of the phosphor layer by the experimental measurement.

Thus, the L_i^B and L_{fs}^{B} in Eq. (4) were derived by the integration of the measured $P_i^B(\lambda)$ and $P_{fs}^{B}(\lambda)$ over the blue-light wavelength region (400-500 nm),

#124178 - $15.00 USD Received 11 Feb 2010; revised 21 May 2010; accepted 7 Jun 2010; published 24 Jun 2010

$$\rho_{fs}^{B-B}(\theta_i,\phi_i,\theta_t,\phi_t)\begin{cases} L_i^B(\theta_i,\phi_i) = \int\limits_{\substack{\text{Blue-light}\\ \text{Region}}} P_i^B(\theta_i,\phi_i,\lambda)d\lambda \\ L_{fs}^B(\theta_t,\phi_t) = \int\limits_{\substack{\text{Blue-light}\\ \text{Region}}} P_{fs}^B(\theta_t,\phi_t,\lambda)d\lambda \end{cases}. \tag{5}$$

Here the spectral BSDFs, $\rho_{fs}^{B\text{-}B}$, can be regarded as the angular spreading function with spectrum dependence.

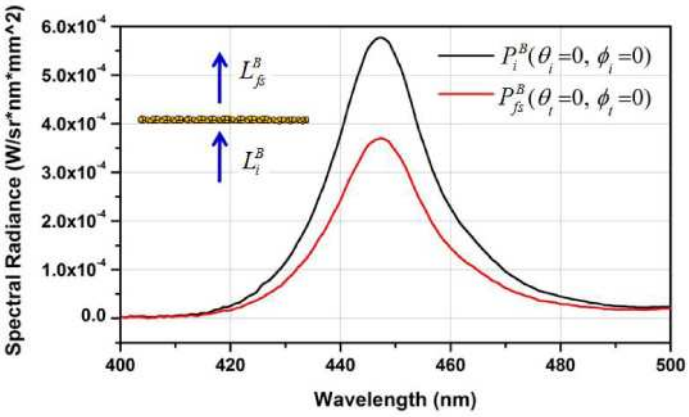

Fig. 2. The normally incident illumination $P_i^B(\lambda)$ and the illumination $P_{fs}^B(\lambda)$ detected in the normal direction

2.3 Blue-to-yellow radiance L_{fe}^Y

The second term on the Eq. (2), L_{fe}^Y, represents the emitted radiance subject to wavelength conversion by the phosphor layer. In general, the converting efficiency of the phosphor is merely determined by the energy-based quantity. As the spatial dependence is considered, a more complete discussion including directional function is included. For pcLEDs, the phosphor-converted efficiency obeys scalability and addictivity due to the unique relation of chip-emitted and phosphor-emitted spectral distribution. The forward emitted radiance L_{fe}^Y can be linearly related to the incident radiance L_i^B and blue-to-yellow bidirectional distribution function $\rho_{fe}^{B\text{-}Y}$,

$$L_{fe}^Y(\theta_t,\phi_t) = \int_{\Omega_i} \rho_{fe}^{B-Y}(\theta_i,\phi_i,\theta_t,\phi_t) L_i^B(\theta_i,\phi_i)\cos\theta_i d\omega_i. \tag{6}$$

where the $\rho_{fe}^{B\text{-}Y}$ is defined as the ratio of the transmitted radiance dL_{fe}^Y in the transmitted direction to the irradiance dE_i^B in an incident direction,

$$\rho_{fe}^{B-Y}(\theta_i,\phi_i,\theta_t,\phi_t) = \frac{dL_{fe}^Y(\theta_t,\phi_t)}{dE_i^B(\theta_i,\phi_i)} = \frac{dL_{fe}^Y(\theta_t,\phi_t)}{L_i^B(\theta_i,\phi_i)\cos\theta_i d\omega_i}, \tag{7}$$

Different from the blue-to-blue radiance, behavior of the forward emitted spectral distribution $P_{fe}^Y(\lambda)$ depends on the phosphor conversion properties. Thus, the $\rho_{fe}^{B\text{-}Y}$ shall be obtained by the wavelength integration over different spectral regions separated by blue (400-500 nm) and yellow (500-750nm), respectively.

#124178 - $15.00 USD Received 11 Feb 2010; revised 21 May 2010; accepted 7 Jun 2010; published 24 Jun 2010

$$\rho_{fe}^{B-Y}(\theta_i,\phi_i,\theta_t,\phi_t)\begin{cases} L_i^B(\theta,\phi) = \int\limits_{\text{Blue-light Region}} P_i^B(\theta,\phi,\lambda)d\lambda \\ L_{fe}^Y(\theta,\phi) = \int\limits_{\text{Yellow-light Region}} P_{fe}^Y(\theta,\phi,\lambda)d\lambda \end{cases}. \quad (8)$$

As a set of the measured spectral radiance distribution in Fig. 3, the emitted spectrum $P_{fe}^{\ Y}(\lambda)$ has a broad spectral distribution over the region of yellow-light. Therefore, the down converting phenomena of the phosphor conversion can be simultaneously described by the dichromatic BSDFs.

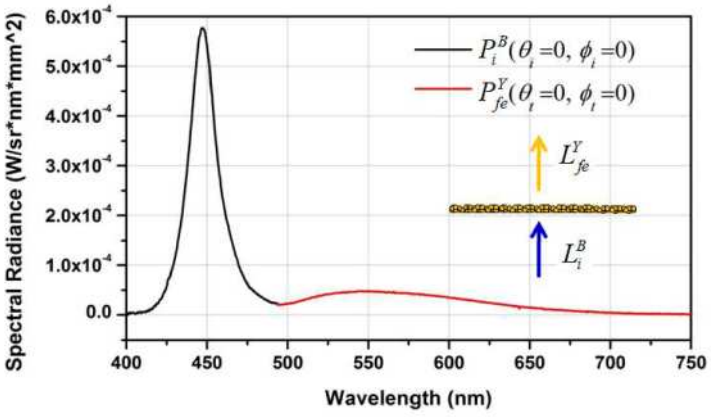

Fig. 3. The normally incident illumination $P_i^{\ B}(\lambda)$ and the illumination $P_{fe}^{\ Y}(\lambda)$ detected in the normal direction

2.4 Yellow-to-yellow radiance $L_{fs}^{\ Y}$

In addition to the incident radiance $L_i^{\ B}$ from GaN LED, the backward phosphor-emitted yellow light can be recycled to induce additional forward scattering in the phosphor layer. To characterize this effect, the non-emitted (scattered) radiance of the energy balance equation Eq. (1) shall take account of recycled radiation, as the third term in Eq. (2). Similar to aforementioned manipulation, the recycling radiance $L_{fs}^{\ Y}$ can be described by the integration of incident light $L_i^{\ Y}$ with the yellow-to yellow bidirectional distribution function $\rho_{fs}^{\ Y\text{-}Y}$

$$L_{fs}^Y(\theta_t,\phi_t) = \int_{\Omega_i} \rho_{fs}^{Y-Y}(\theta_i,\phi_i,\theta_t,\phi_t) L_i^Y(\theta_i,\phi_i)\cos\theta_i d\omega_i, \quad (9)$$

where $\rho_{fs}^{\ Y\text{-}Y}$ is defined by

$$\rho_{fs}^{Y-Y}(\theta_i,\phi_i,\theta_t,\phi_t) = \frac{dL_{fs}^Y(\theta_t,\phi_t)}{dE_i^Y(\theta_i,\phi_i)} = \frac{dL_{fs}^Y(\theta_t,\phi_t)}{L_i^Y(\theta_i,\phi_i)\cos\theta_i d\omega_i}. \quad (10)$$

As the blue-to-blue bidirectional distribution function $\rho_{fs}^{\ B\text{-}B}$ introduced in Section 2.2, the $\rho_{fs}^{\ Y\text{-}Y}$ is obtained by the integrations of the spectral distributions $P_i^{\ Y}(\lambda)$ and $P_{fs}^{\ Y}(\lambda)$ over the yellow-light region (500-750 nm),

$$\rho_{fs}^{Y-Y}(\theta_i,\phi_i,\theta_t,\phi_t)\begin{cases} L_i^Y(\theta,\phi) = \int\limits_{\text{Yellow-light Region}} P_i^Y(\theta,\phi,\lambda)d\lambda \\ L_{fs}^Y(\theta,\phi) = \int\limits_{\text{Yellow-light Region}} P_{fs}^Y(\theta,\phi,\lambda)d\lambda \end{cases}. \quad (11)$$

#124178 - $15.00 USD Received 11 Feb 2010; revised 21 May 2010; accepted 7 Jun 2010; published 24 Jun 2010

A sample of the measured spectral distributions $P_i^Y(\lambda)$ and $P_{fs}^Y(\lambda)$ were conducted, as shown in Fig. 4. It is important to note that the spectral BSDFs are highly relevant to the phosphor recipes, wavelength and illumination/viewing geometry. Different specimens and illuminating sources would exhibit discrepant BSDFs.

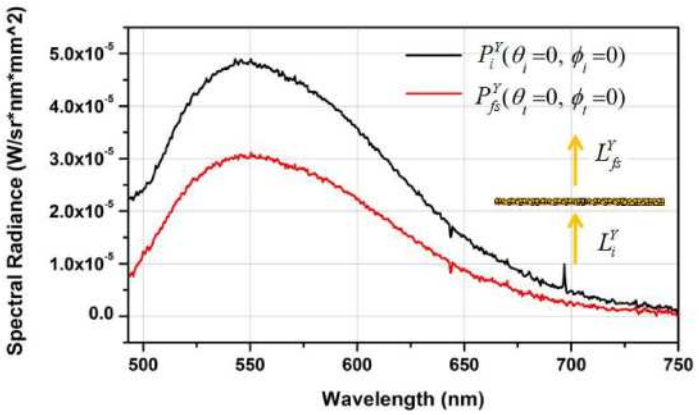

Fig. 4. The normally incident illumination $P_i^Y(\lambda)$ and the illumination $P_{fs}^Y(\lambda)$ detected in the normal direction

2.5 Radiance integration

To summarize the aforementioned manipulation about phosphor characterization, the spectral BSDFs were contributed by the three independent components: $\rho_{fs}^{B\text{-}B}$, $\rho_{fe}^{B\text{-}Y}$, and $\rho_{fs}^{Y\text{-}Y}$.

$$\rho(\theta_i,\phi_i,\theta_t,\phi_t) = \rho_{fs}^{B-B}(\theta_i,\phi_i,\theta_t,\phi_t) + \rho_{fe}^{B-Y}(\theta_i,\phi_i,\theta_t,\phi_t) + \rho_{fs}^{Y-Y}(\theta_i,\phi_i,\theta_t,\phi_t), \quad (12)$$

In additional to the dichromatic white mixing scheme, proposed methodology can be extended to a general form subject to the multiple excitation radiance,

$$\rho(\theta_i,\phi_i,\theta_t,\phi_t) = \rho_{fs}^{\lambda_0-\lambda_0}(\theta_i,\phi_i,\theta_t,\phi_t) + \sum_m (\rho_{fe}^{\lambda_0-\lambda_m}(\theta_i,\phi_i,\theta_t,\phi_t) + \rho_{fs}^{\lambda_m-\lambda_m}(\theta_i,\phi_i,\theta_t,\phi_t)), \quad (13)$$

where λ_0 is the wavelength of the light source, such as the blue light from the GaN LEDs. The index *m* represents *m*-th emitted spectrum which depends on the light source and the converting properties of the phosphor.

Through the characterizations of the spectral BSDFs, the transmitting-side optical properties of a phosphor layer in a pcLED can be numerically obtained by the integration (Eq. (2).) Several studies have been proposed to tackle the radiance integration [15, 16]. Among the various approaches, the Monte Carlo method is most common and available from the commercial simulation tools [14]. Here we used a Monte Carlo method based computational tool, LightTools, to implement the integration.

3. Experiment

3.1 BSDFs measurement

The spectral BSDFs of a YAG phosphor layer were measured by the conoscopic approach associated with an in-house light source module [17,18]. Because of the rotationally symmetric properties of the YAG phosphor layer, the two-dimensional illumination sampling for the BSDFs measurement can be reduced to one-dimensional illumination scanning. As the schematic illustration in Fig. 5(a), the specimen was illuminated by a collimated beam with a set of discrete incident directions θ_i, and the corresponding angular spread function can be collected by the objective lens with the moderate numerical aperture for the observation of the imaged plane. The definition of the spectral BSDF is a ratio of differentials, so the basic

#124178 - $15.00 USD Received 11 Feb 2010; revised 21 May 2010; accepted 7 Jun 2010; published 24 Jun 2010

problem with practical measurement lies on the instrument angular resolution. Here the in-house collimated source, which the divergent angle is limited within ± 1 degree, was equipped to illuminate the phosphor surface from each incident angle. We used illumination aperture of 2-mm diameter to measure BSDF. Detailed discussions can refer to the literature [15]. Figure 5(b) shows one set of the measured angular spread functions of a test specimen with the different incident angles θ_i along a constant azimuthal direction ϕ_i = 90°. Every incident beam illuminating the specimen would lead to an angular spread function. As the measured BSDFs vary smoothly under different incident angles θ_i, the angular sampling is adequate to completely characterize the scattering behavior. The BSDFs are highly relevant to the geometric natures of the phosphor particulates.

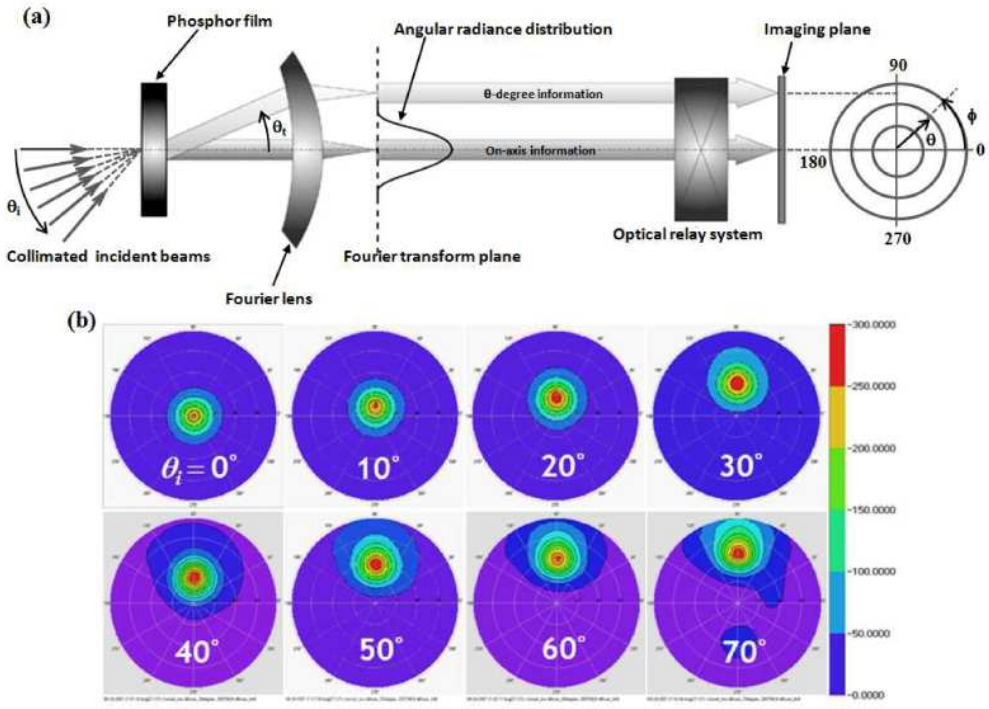

Fig. 5. (a) Schematic measurement setup of BSDFs, (b) the measured angular spread functions of an available specimen.

In order to obtain the spectral BSDFs ρ in Eq. (12), three components were individually measured. First of all, the collimated incident beams with the designated spectral radiance distributions $P_i^B(\lambda)$ or $P_i^Y(\lambda)$ was set to illuminate the YAG phosphor film, where phosphor was coated on a thin substrate with identical coating parameters. Then, the spectrophotometric measurement was executed by scanning over the imaging plane of the conoscopic system to obtain the corresponding spectral radiance distribution, $P_{fs}^B(\theta_t,\phi_t,\lambda)$, $P_{fe}^Y(\theta_t,\phi_t,\lambda)$, $P_{fs}^Y(\theta_t,\phi_t,\lambda)$, accordingly. Figure 6 shows the measured results of $P_{fs}^B(\theta_t,\lambda)$ and $P_{fe}^Y(\theta_t,\lambda)$, where the spectrometer scanned over the θ_t direction with 5-degree intervals under the normal illumination condition of the blue LED source. Based on the definition of dichromatic BSDF, the scattered and the emitted angular spread function can be separated by the integration boundary of the measured spectral distributions. Figure 7(a)-(c) show the measured $\rho_{fs}^{B\text{-}B}$, $\rho_{fe}^{B\text{-}Y}$, and $\rho_{fs}^{Y\text{-}Y}$ of the considered phosphor film. In addition to the forward radiance in the transmitting hemisphere of the phosphor layer, the backward components, $\rho_{bs}^{B\text{-}B}$, $\rho_{be}^{B\text{-}Y}$, and $\rho_{bs}^{Y\text{-}Y}$, can be obtained via the same procedure as well.

The spectral BSDFs also provide a figure of merit to qualitatively examine the optical properties of the phosphor film. The spectral BSDFs are highly dependent on the recipe and

#124178 - $15.00 USD Received 11 Feb 2010; revised 21 May 2010; accepted 7 Jun 2010; published 24 Jun 2010

micro-feature of the phosphor layer, different manufactures will have their own BSDFs. In this case, the transmitted angular distribution in Fig.7 (a) and (c) is concentrated in a relatively narrow angular range with shift variant properties. On the other hand, blue-to-yellow bidirectional distribution functions in Fig.7 (b) implies the wavelength conversion mechanism effectively leave the YAG phosphor layer as a near Lambertian field.

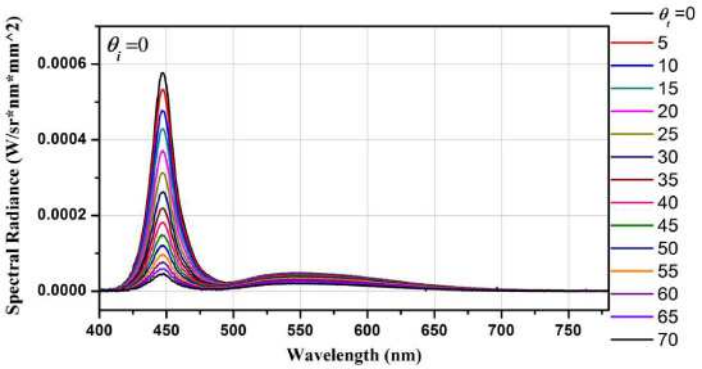

Fig. 6. The measured results of $P_{fs}^{B}(\theta_i,\lambda)$ and $P_{fe}^{Y}(\theta_i,\lambda)$ under normal illuminatio

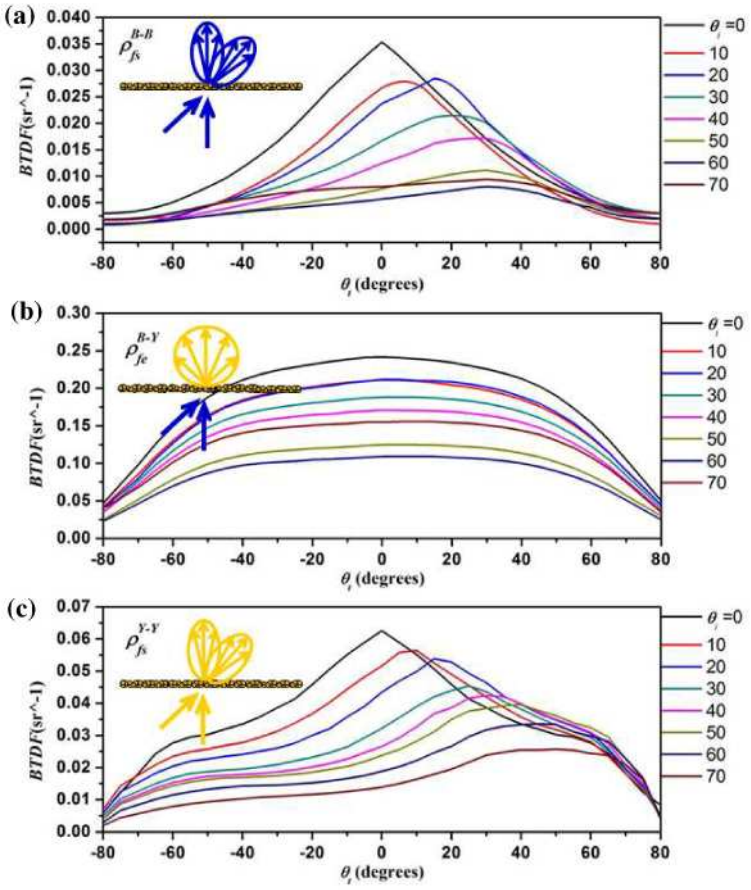

Fig. 7. The measured (a) $\rho_{fs}^{B\text{-}B}$, (b) $\rho_{fe}^{B\text{-}Y}$, and (c) $\rho_{fs}^{Y\text{-}Y}$ of the considered phosphor

#124178 - $15.00 USD Received 11 Feb 2010; revised 21 May 2010; accepted 7 Jun 2010; published 24 Jun 2010

3.2 Verification

In order to validate the phosphor characterization, a commercially available pcLED with conformal phosphor coating was examined. Firstly, the BSDF measurement of the YAG phosphor coated on PET substrate was conducted, where the coating method and recipe of the phosphor were identical to that in chip-level. Then we imported the measured bidirectional photometric data (in Section 3.1) into the simulation with GaN blue LED chip (0.5 × 0.5 mm^2) to predict both blue and yellow radiant intensity distribution. The inset of Fig. 8 shows the measured pcLED, where the phosphor coated on the blue LED chip (0.5 × 0.5 mm) was fabricated by the pulsed spray coating method [19]. Because of the consideration of the multi-wavelength emission, the simulation was performed in multi-steps. After summing the simulated results of each wavelength, the simulated far-field luminous intensity distribution and angular correlated color temperature (CCT) distribution are shown in Fig. 8(a) and (b), respectively [20]. Comparing with the experimental measurements, the numerical predictions have 98.9% and 97.9% correlation with the practical results. The CCT deviations are mainly resulted from the BSDF measurement errors attributed by the distortion of conoscopic system. After the energy superposition of Eq. (2), the BSDF errors would be cumulated. Despite the deviations, the simulated CCT distribution curve still provides useful information to evaluate the color uniformity of a pcLED configuration. The close agreement of the measurement demonstrated the validity of the proposed model for phosphor description in the pcLED applications.

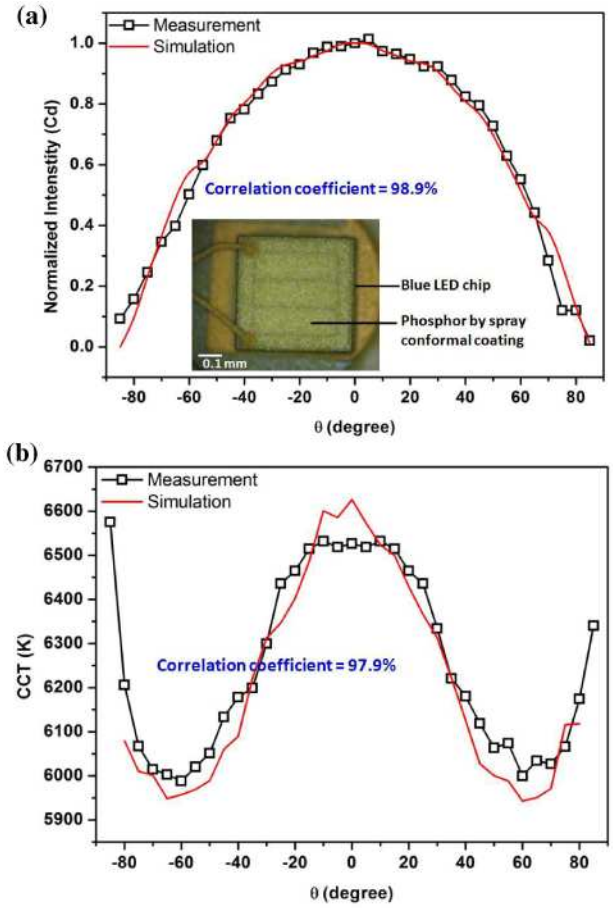

Fig. 8. The simulated (a) luminous intensity distribution and (b) angular CCT distribution

#124178 - $15.00 USD Received 11 Feb 2010; revised 21 May 2010; accepted 7 Jun 2010; published 24 Jun 2010

4. Conclusions

A simple but effective phosphor modeling of the pcLED is proposed. The major advantage of this study lies in that there is no need to formulate the complex physical mechanism of the phosphor scattering in a microscopic viewpoint. Instead, as long as the coated phosphor layer is available, the proposed methodology assisted by the measured BSDFs is able to characterize the phosphor properties with the direction and wavelength variables. By the Monte Carlo simulation, pcLED luminous intensity distribution and its angular CCT distribution can be predicted with high accuracy. Closed agreement with a commercially available pcLED validates the proposed scheme, which certainly has impact for the LED development in illumination applications.

Acknowledgment

The authors thank Bo-Wen Xiao, Hsin-Tao Huang and Yi-Pai Huang for helpful discussions and experimental support. The financial support from National Science Council, Taiwan, under contract NSC 96-2221-E-009-114-MY3 is also acknowledged.

#124178 - $15.00 USD Received 11 Feb 2010; revised 21 May 2010; accepted 7 Jun 2010; published 24 Jun 2010